PALEOCEANOGRAPHY, VOL. 28, 164–174, doi:10.1002/palo.20018, 2013

Seasonal patterns of shell flux, $\delta^{18}O$ and $\delta^{13}C$ of small and large *N. pachyderma* (s) and *G. bulloides* in the subpolar North Atlantic

Lukas Jonkers,[1,2] Steven van Heuven,[3] Rainer Zahn,[4] and Frank J.C. Peeters[5]

Received 5 November 2012; revised 28 January 2013; accepted 2 February 2013; published 25 March 2013.

[1] Past water column stratification can be assessed through comparison of the $\delta^{18}O$ of different planktonic foraminiferal species. The underlying assumption is that different species form their shells simultaneously, but at different depths in the water column. We evaluate this assumption using a sediment trap time-series of *Neogloboquadrina pachyderma* (s) and *Globigerina bulloides* from the NW North Atlantic. We determined fluxes, $\delta^{18}O$ and $\delta^{13}C$ of shells from two size fractions to assess size-related effects on shell chemistry and to better constrain the underlying causes of isotopic differences between foraminifera in deep-sea sediments. Our data indicate that in the subpolar North Atlantic differences in the seasonality of the shell flux, and not in depth habitat or test size, determine the interspecies $\Delta\delta^{18}O$. *N. pachyderma* (s) preferentially forms from early spring to late summer, whereas the flux of *G. bulloides* peaks later in the season and is sustained until autumn. Likewise, seasonality influences large and small specimens differently, with large shells settling earlier in the season. The similarity of the seasonal $\delta^{18}O$ patterns between the two species indicates that they calcify in an overlapping depth zone close to the surface. However, their $\delta^{13}C$ patterns are markedly different (>1‰). Both species have a seasonally variable offset from $\delta^{13}C_{DIC}$ that appears to be governed primarily by temperature, with larger offsets associated with higher temperatures. The variable offset from $\delta^{13}C_{DIC}$ implies that seasonality of the flux affects the fossil $\delta^{13}C$ signal, which has implications for reconstruction of the past oceanic carbon cycle.

Citation: Jonkers, L., S. van Heuven, R. Zahn, and F. J. C. Peeters (2013), Seasonal patterns of shell flux, $\delta^{18}O$ and $\delta^{13}C$ of small and large *N. pachyderma* (s) and *G. bulloides* in the subpolar North Atlantic, *Paleoceanography*, *28*, 164–174, doi:10.1002/palo.20018.

1. Introduction

[2] Differences in the depth or seasonal habitat between planktonic foraminiferal species can lead to differences in the geochemical composition of their shells. In principle, the stable oxygen isotope contrast ($\Delta\delta^{18}O$) between two (or more) species can therefore be used to infer past upper water column stratification [*Hillaire-Marcel et al*., 2001; *Mulitza et al*., 1997]. However, this approach requires a detailed knowledge of the controls on stable isotope incorporation, the depth habitat, and the seasonal signal recorded in foraminiferal calcite, particularly because foraminifera are able to change their spatial and temporal habitat preferences [*Field*, 2004; *Tolderlund and Bé*, 1972]. Furthermore, distinguishing between the effects of depth and seasonality on the fossil interspecies $\Delta\delta^{18}O$ is nontrivial and different authors have interpreted the $\Delta\delta^{18}O$ between the same species to reflect either seasonality [*Jonkers et al*., 2010a] or depth habitat differences [*Simstich et al*., 2003].

[3] The $\delta^{13}C$ of the dissolved inorganic carbon (DIC) in seawater is the product of various interfering fractionation processes, with nutrient cycling and air-sea CO_2 exchange probably the most important [*Broecker and Peng*, 1982; *Broecker and Maier-Reimer*, 1992]. The $\delta^{13}C$ of planktonic foraminiferal species is often used as a proxy for changes in the $\delta^{13}C$ of DIC and therefore the carbon cycle. However, foraminiferal $\delta^{13}C$ can be offset from $\delta^{13}C_{DIC}$ due to various biological, physical, and chemical processes, commonly referred to with the broad term vital effects. The most important vital effects are (i) ontogenetic/metabolic effects, (ii) photosynthetic activity by symbionts, (iii) temperature, and (iv) carbonate system parameters [e.g., *Bemis et al*., 2000; *Peeters et al*., 2002; *Ravelo and Fairbanks*, 1995; *Spero et al*., 1997]. Compared to oxygen isotopes, the controls on the incorporation of $\delta^{13}C$ into foraminiferal calcite are much less

All Supporting Information may be found in the online version of this article.

[1]Institut de Ciència i Tecnologia Ambientals (ICTA), Universitat Autònoma de Barcelona, Campus UAB, Bellaterra (Cerdanyola del Vallès), Spain.

[2]Now at School of Earth and Ocean Sciences, Cardiff University, Cardiff, UK.

[3]Center for Isotope Research, University of Groningen, Groningen, The Netherlands.

[4]Institució Catalana de Recerca i Estudis Avançats (ICREA), Institut de Ciència i Tecnologia Ambientals (ICTA), Departament de Física, Universitat Autònoma de Barcelona, Bellaterra, Spain.

[5]Faculty of Earth and Life Sciences (FALW), Vrije Universiteit Amsterdam, Amsterdam, The Netherlands.

Corresponding author: L. Jonkers, Cardiff University, School of Earth and Ocean Sciences, Park place, Cardiff CF10 3AT, UK. (jonkersl@cardiff.ac.uk)

0883-8305/13/10.1002/palo.20018

well constrained, limiting the applicability of foraminiferal $\delta^{13}C$ in paleoceanographic research.

[4] Both oxygen and carbon isotopes have been shown to be dependent on foraminiferal shell size [e.g., *Berger et al*., 1978; *Billups and Spero*, 1995; *Bouvier-Soumagnac and Duplessy*, 1985]. In foraminifera preserved in the sediment, size-dependent differences reflect the combined effects of ontogeny, seasonality and depth habitat [e.g., *Deuser et al*., 1981; *Kuroyanagi et al*., 2011; *Peeters et al*., 2002]. However, if the ontogenetic effect is known, and this may be deduced using sediment traps, the residual isotope difference between different-sized foraminifera can be better constrained. Additionally, in the case of $\delta^{18}O$, this difference can potentially be used as an indicator of thermal water column stratification [*Kuroyanagi et al*., 2011]. A better understanding of the dependence of stable isotope composition on shell size and foraminiferal species can therefore improve the accuracy of inferences of past oceanographic conditions. To that purpose, we explore in this paper the effects of seasonality and shell size on the stable oxygen and carbon isotope composition of left-coiling *Neogloboquadrina pachyderma* sinistral (s) and *Globigerina bulloides* using a moored sediment trap time series across 2.5 seasonal cycles from the subpolar North Atlantic.

1.1. Seasonal Hydrography

[5] The hydrography of the study site in the central Irminger Sea (Figure 1) has been extensively discussed previously; see *Jonkers et al*. [2010a]. Briefly, the upper 200 m of the water column in the Irminger Gyre is characterized by sea surface temperatures between 5 and 10°C, sea surface salinities between 34.92 in winter and 34.65 in summer, and a wind-mixed layer of approximately 50 m deep during summer (Figure 1B). Below about 200 m temperature and salinity are virtually constant throughout the year around 5°C and 34.9, respectively (Figure 1B). During winter, the entire water column is well mixed down to depths of >1 km, allowing for occasional deep convection and formation of deep water [*Bacon et al*., 2003].

2. Methodology

2.1. Sediment Trap

[6] We use a 2.5 year time series (2003–2004 and 2005–2007) of settling flux from sediment traps moored at 2750 m depth (250 m above the seafloor) in the central Irminger Sea (59°N, 39°W; Figure 1). Collection cups, poisoned with $HgCl_2$ to ensure sample preservation, were rotated every 19 or 16 days. A full description of the sediment trap set-up is given in *Jonkers et al*. [2010a]. To compensate for production and settling offsets, all flux data have been shifted backward by one month.

2.2. Foraminiferal Analyses

[7] Shells of *N. pachyderma* (s) and *G. bulloides* were counted and picked from two sieved size fractions commonly used in paleoceanographic studies: 150–250 μm (small) and 250–315 μm (large). Data on small *N. pachyderma* (s) were reported earlier [*Jonkers et al*., 2010a]. Foraminiferal analyses were carried out on half of the original sample (1/2 split). Shell counts were performed on these sample halves, or on further binary splits when the number of shells exceeded 200. For stable isotope analyses, a minimum of 20, but generally 40 shells were used. Prior to analysis, shells were cracked open between clean glass plates and repeatedly cleaned ultrasonically with milli-Q and MeOH. Measurements were conducted on a Thermo MAT 253 IR-MS coupled to a Kiel IV device at the Universitat Autònoma de Barcelona, Spain. Long-term precision, based on repeated measurements of NBS19 and IAEA CO1, is 0.05 for $\delta^{18}O$ and 0.03‰ for $\delta^{13}C$ (1 σ). To ensure consistency between the new data presented here and those of *Jonkers et al*. [2010a], 15 samples of small *N. pachyderma* (s) were also analyzed at the Universitat Autònoma de Barcelona. Results from both mass spectrometers are statistically indistinguishable, thus data from the two studies can be confidently compared. The flux and stable isotope data are available at http://doi.pangaea.de/10.1594/PANGAEA.807458.

2.3. Water Column Data

[8] Daily satellite-derived sea surface temperature data (L4 AVHRR_OI) were obtained from GODAE High Resolution Sea Surface Temperature Pilot Project (accessed via http://podaac.jpl.nasa.gov). To compensate for the sparse spatial and temporal sea surface salinity observations, a composite salinity curve was constructed using data from the Global Temperature-Salinity Profile Program [*Jonkers et al*., 2010a]. In situ temperature and salinity measurements at 200 m depth were made daily with a nearby moored CTD-profiler (site "loco" in Figure 1) and vertical hydrographic profiles were obtained annually when the mooring was serviced [*Jonkers et al*., 2010a]. Temperature and salinity were converted to equilibrium $\delta^{18}O$ ($\delta^{18}O_{eq}$) using a linear relationship between salinity and seawater $\delta^{18}O$ [$\delta^{18}O_W = 0.5417 * S - 18.767$; *Jonkers et al*., 2010a], converted to the VPDB scale by subtracting 0.27 ‰ [*Hut*, 1987] and using the *Kim and O'Neil* [1997] equation

$$T\,(^{\circ}\mathrm{C}) = 16.10 - 4.64\left(\delta^{18}O_c - \delta^{18}O_w\right) + 0.09\left(\delta^{18}O_c - \delta^{18}O_w\right)^2 \quad (1)$$

where $\delta^{18}O_c$ and $\delta^{18}O_w$ are the $\delta^{18}O$ of calcite and water, respectively.

[9] Due to the extreme scarcity of measurements, the seasonal cycle of $\delta^{13}C_{DIC}$ and carbonate ion concentration ($[CO_3^{2-}]$) in the mixed layer were estimated from hydrographical data from the wider North Atlantic using a multiple linear regression (MLR) approach. Data were assembled from the GLODAP [*Key et al*., 2004] and CARINA [*Key et al*., 2010] data sets. Data from cruise 64TR19900417 (R/V *Tyro*, 1990) were excluded, as $\delta^{13}C_{DIC}$ values were suspiciously low and variable, likely as a result of incomplete extraction of CO_2 from the samples. To enhance coverage data from the 1981 TTO-NAS cruise, obtained through CDIAC (http://cdiac.esd.ornl.gov/ftp/oceans/keeling.data/) were added. The resulting combined data set contains approximately 250 values of $\delta^{13}C_{DIC}$ in the upper 500 m of the North Atlantic Ocean (between 50°N and 65°N; see Figure S1 in the Supporting Information). All $\delta^{13}C$ values were "time-shifted" to 2007 using the −0.018‰/yr rate determined by *Quay et al*. [2007] to compensate for the ongoing decrease in $\delta^{13}C_{DIC}$ due the uptake by the ocean of (low-$\delta^{13}C$) fossil fuel derived CO_2.

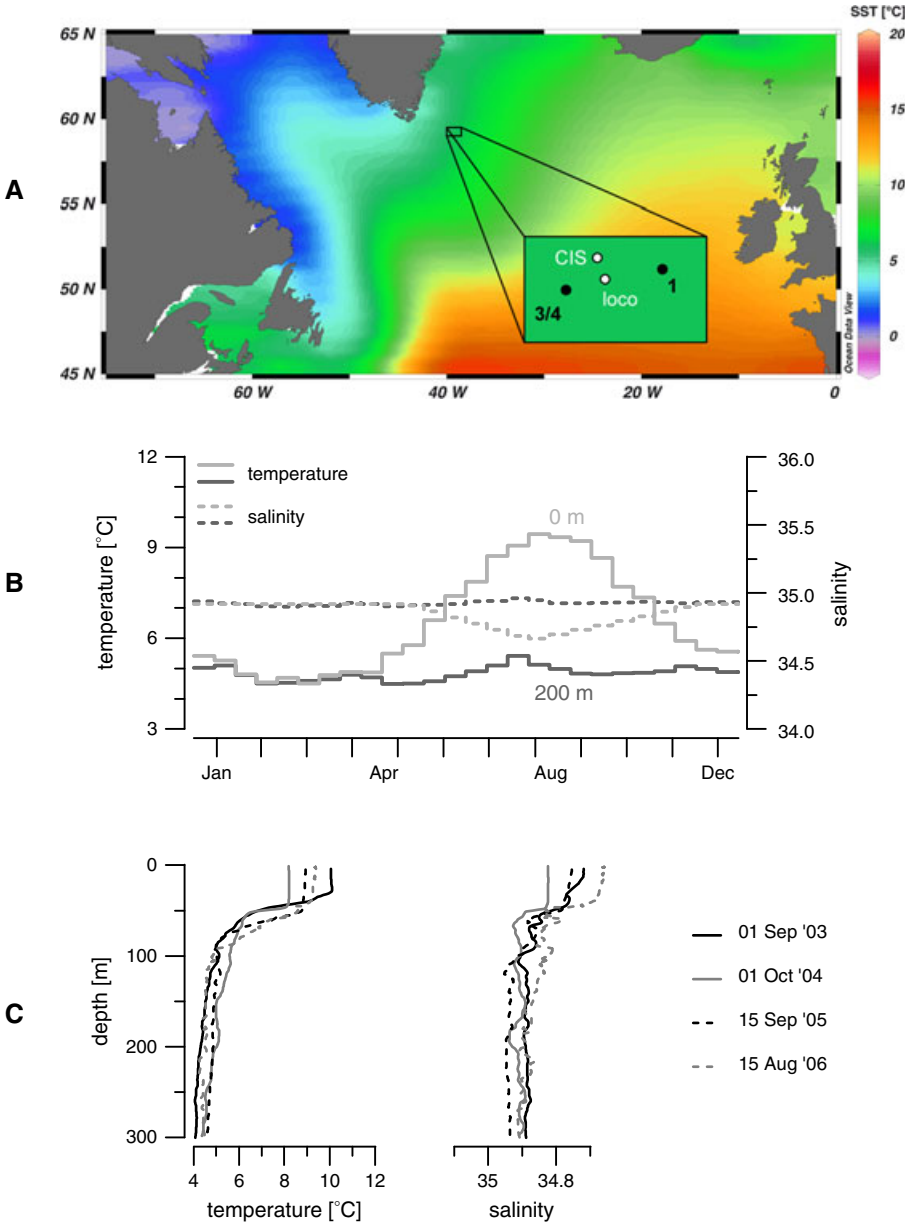

Figure 1. Location of the sediment trap mooring and local hydrography. (A) Contoured mean annual sea surface temperature in the northern North Atlantic [*Locarnini et al*., 2010] and position of the moorings. The black numbers in the blow-up refer to the moored sediment trap: 1 is 2003–2004, 3/4 is 2005–2007. Temperature and salinity data at 200 m depth are from the LOCO mooring and mixed layer nitrate concentrations from the CIS mooring. (B) Biweekly averaged temperature and salinity at 0 and 200 m depth. (C) In situ temperature and salinity profiles (B and C after *Jonkers et al*. [2010a]).

[10] Next, using MLR, a predictive relationship for DIC was established using concurrent observations ($n = 1139$) of DIC and temperature, salinity and NO_3^- in the region between 53°N–65°N; 45°W–34°W; 0–450 m (this region was deemed the optimal compromise between the desire to (i) include as much data as is available and (ii) maximize its representativeness of our study site). For alkalinity, an identically set up MLR was performed ($n = 929$) to allow for the calculation of $[CO_3^{2-}]$ later on. Third, for $\delta^{13}C_{DIC}$ an MLR was performed (albeit in a larger region due to data scarcity: 45°N–68°N; 80°W–10°E; 0–450 m) using temperature, salinity, NO_3^- and (observed) DIC as predictive properties ($n = 134$). Performance of these MLRs appears satisfactory (see Figure S2 and equations in the Supporting Information): the root-mean-square error of the residuals between predicted and observed DIC, ALK, and $\delta^{13}C_{DIC}$ are 6.9 and 5.2 µmol/kg and 0.12‰, respectively.

[11] Using the obtained MLR coefficients, values of DIC^{MLR}, ALK^{MLR}, and $\delta^{13}C_{DIC}{}^{MLR}$ were calculated from (i) monthly mean values for S, T, and NO_3^- from the World Ocean Atlas 2009 (WOA09) [*Antonov et al*., 2010; *Garcia et al*., 2010; *Locarnini et al*., 2010] for the region around

the sediment trap (57°N to 61°N; 41°W to 37°W; 0–35 m) and (ii) from in situ observations (at near daily resolution) from September 2003 to May 2004 from the CIS mooring (59.6°N; 39.6°W; 30–40 m; data obtained through www.eurosites.info/cis/data.php). Calculation of $\delta^{13}C_{DIC}^{MLR}$ required the additional use of DIC^{MLR} as an input variable.

[12] As may be expected, the predicted values of $\delta^{13}C_{DIC}$ of surface waters (0–35 m) in wintertime closely resemble the values observed in summer at depths below the stratified, euphotic surface layer at around 0.75‰. The estimated seasonal amplitude of $\delta^{13}C_{DIC}$ at the surface (0–35 m) of approximately 0.5‰ is comparable to literature values for the North Atlantic (0–50 m) [*Gruber et al.*, 1999], further strengthening the case for the appropriateness of this approach.

[13] Lastly, the seasonal cycle of $[CO_3^{2-}]$ was calculated from DIC^{MLR} and ALK^{MLR} using CO2SYS for MATLAB [*van Heuven et al.*, 2009].

3. Results

[14] The time series data are presented first as raw data for the entire period and second as one-year composites with biweekly averages.

3.1. Shell Fluxes

[15] The flux of small *N. pachyderma* (s) is by far the highest with maxima reaching 1843 shells/m^2/d during spring 2007 (Figure 2). The flux appears to be characterized by a bimodal pattern, with a first pulse in April–May and a second, of approximately equal magnitude, in August–September (Figure 2). From December to the end of March settling fluxes are close to zero (Figure 2). Large *N. pachyderma* (s) have fluxes that are an order of magnitude lower and predominantly settle earlier in the season than the small ones (Figure 2). The settling flux of large *N. pachyderma* (s) starts approximately 2 weeks after that of the small shells of this species, and fluxes decline to zero from as early as mid-July (Figure 2).

[16] In *G. bulloides* the difference in the magnitude of the settling fluxes between the size classes is less pronounced than in *N. pachyderma* (s), with the flux of small shells only slightly higher (Figure 2). The fluxes of both size classes have a unimodal shape and arrive between April and December: small *G. bulloides* with a maximum between August and October and large *G. bulloides*, with an earlier maximum from June to August (Figure 2).

3.2. Oxygen Isotopes

[17] Stable oxygen isotopes of small *N. pachyderma* (s) vary in concert with the predicted sea surface $\delta^{18}O_{eq}$ between 0.93 and 2.63‰; values below sea surface $\delta^{18}O_{eq}$ only occur after the autumn flux pulse (Figure 3). Large *N. pachyderma* (s) $\delta^{18}O$ values range between 1.62 and 2.75‰ and follow the same pattern as the small shells without any significant offset (mean 0.04 ± 0.10‰; Figure 3).

[18] The $\delta^{18}O$ of *G. bulloides* also closely follows the seasonal $\delta^{18}O_{eq}$ cycle (Figure 3). Small shells vary between 0.87 and 2.46‰ and the large ones between 1.34 and 2.65‰ (Figure 3). However, contrary to *N.*

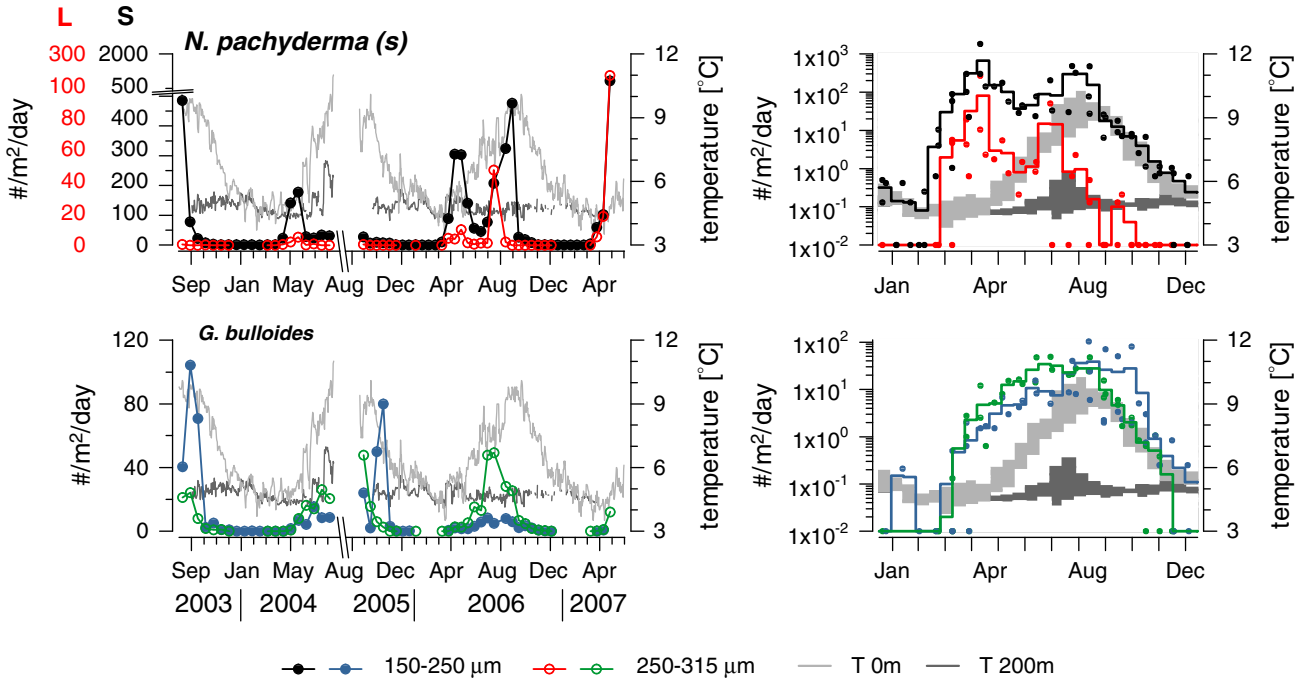

Figure 2. Shell fluxes of *N. pachyderma* (s) and *G. bulloides*. Left-hand panels show the complete time series compared to seawater temperature at 0 and 200 m depth. Symbols indicate midpoints of the 19 (2003–2004) to 16 (2005–2007) days collecting intervals. Right-hand panels show annually stacked data (colored points) and biweekly averaged values (thick lines). In the right-hand panels zero fluxes are plotted as 0.01. Biweekly temperature ranges ($\pm$ 1 σ) are shown in grey. Note the different scales of the flux axes for both species.

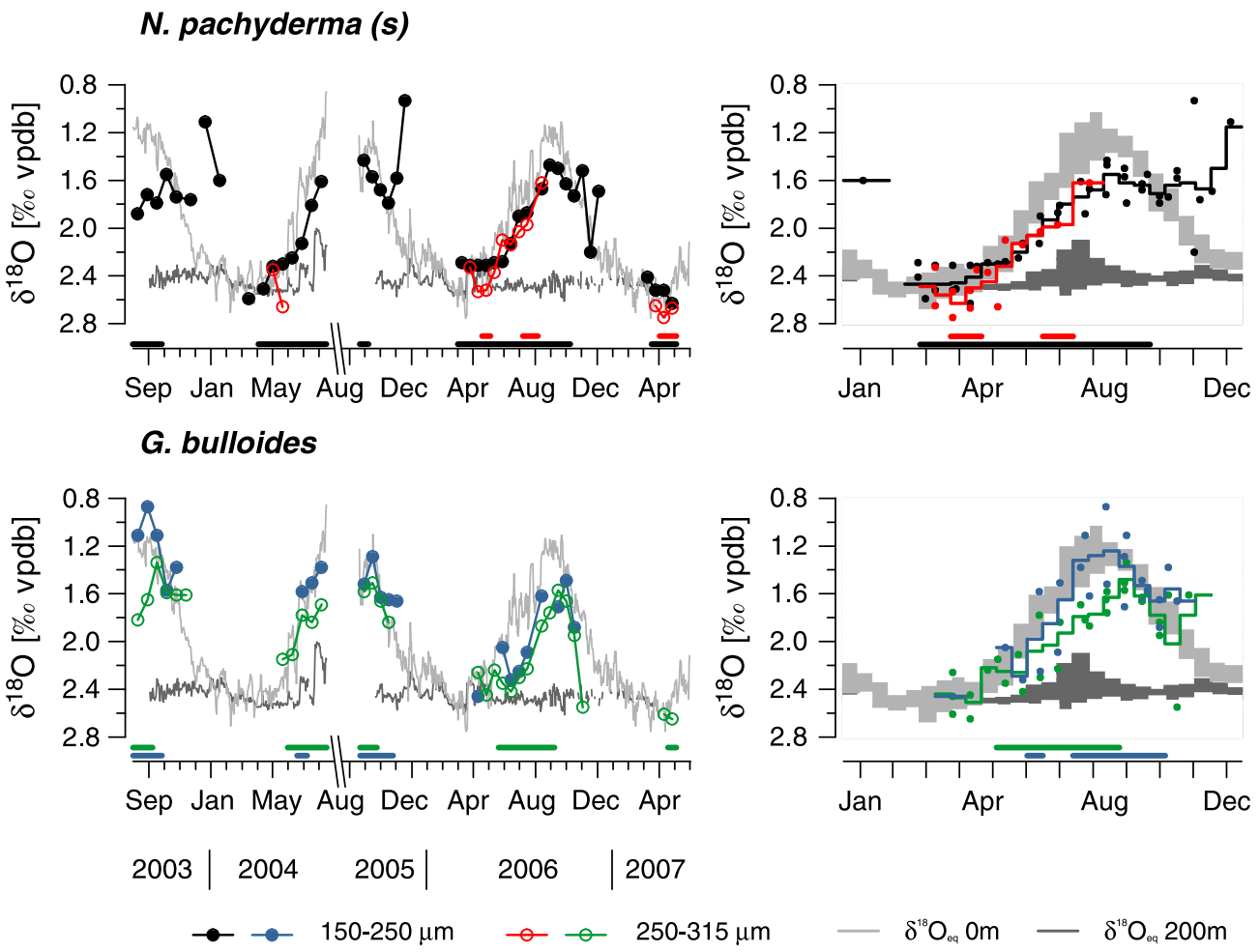

Figure 3. Stable oxygen isotopes of *N. pachyderma* (s) and *G. bulloides* compared to equilibrium $\delta^{18}O$ calculated using the 0 and 200 m temperature and salinity shown in Figure 1B and equation (1). Lay out of the plots follows Figure 2. Thick horizontal lines just above the *x*-axis indicate periods when the shell fluxes were $\geq 10/m^2/d$. Both species' $\delta^{18}O$ overlap with $\delta^{18}O_{eq}$ in late winter/early spring when the water column is mixed, indicating calcification in accordance with equilibrium.

pachyderma (s), the difference between the size classes is larger in *G. bulloides*, with the small shells having on average 0.20 ± 0.18‰ lower $\delta^{18}O$. This difference varies interannually and appears larger during sea surface temperature maxima, when the small shells have lower $\delta^{18}O$ than large shells (Figure 3).

[19] Because the water column is deeply mixed between December and May, $\delta^{18}O_{eq}$ values are identical at all depths during these months (Figure 3). Thus, the offset from equilibrium calcification can be determined for shells formed during this period without making an assumption on the depth habitat of the species. For both *N. pachyderma* (s) and *G. bulloides* and for both size classes the $\delta^{18}O$ values overlap with the predicted $\delta^{18}O_{eq}$ from March to early May, indicating that they all precipitate calcite in accordance with inorganic calcification (Figure 3).

3.3. Carbon Isotopes

[20] The $\delta^{13}C$ of small *N. pachyderma* (s) varies seasonally between -0.29 and 0.49‰ (Figure 4A). Values generally increase rapidly from March to early May and then slowly decrease during the rest of the year (Figure 4A). Large shells of this species have slightly higher $\delta^{13}C$ values (0.12 ± 0.04‰) than small shells, and although the time series is shorter, the $\delta^{13}C$ pattern of the large and small shells is similar (Figure 4A).

[21] *G. bulloides* $\delta^{13}C$ values are considerably lower than *N. pachyderma* (s) and there is a larger, but more variable, difference between the two size fractions (0.28 ± 0.21‰). Small *G. bulloides* $\delta^{13}C$ values vary between -0.53 and -1.56‰ and large between -0.31 and -1.21‰ (Figure 4C). Interannual variability is considerable, but a pattern similar, although delayed relative to *N. pachyderma* (s) is observed with the switch to higher $\delta^{13}C$ values in June for the small and in July for the large shells (Figure 4C).

[22] Both species show an offset from mixed layer $\delta^{13}C_{DIC}$ ($\delta^{13}C_{cal\text{-}DIC}$) that changes during the season (Figures 4B and 4D). *N. pachyderma* (s) $\delta^{13}C$ is always closer to $\delta^{13}C_{DIC}$ than *G. bulloides* (mean offsets -0.81 and -1.97‰ for *N. pachyderma* (s) and *G. bulloides*, respectively). In both species the $\delta^{13}C_{cal\text{-}DIC}$ increases toward the sea surface temperature maximum and is more variable when fluxes are low in the autumn (Figures 4B and 4D). The offset from

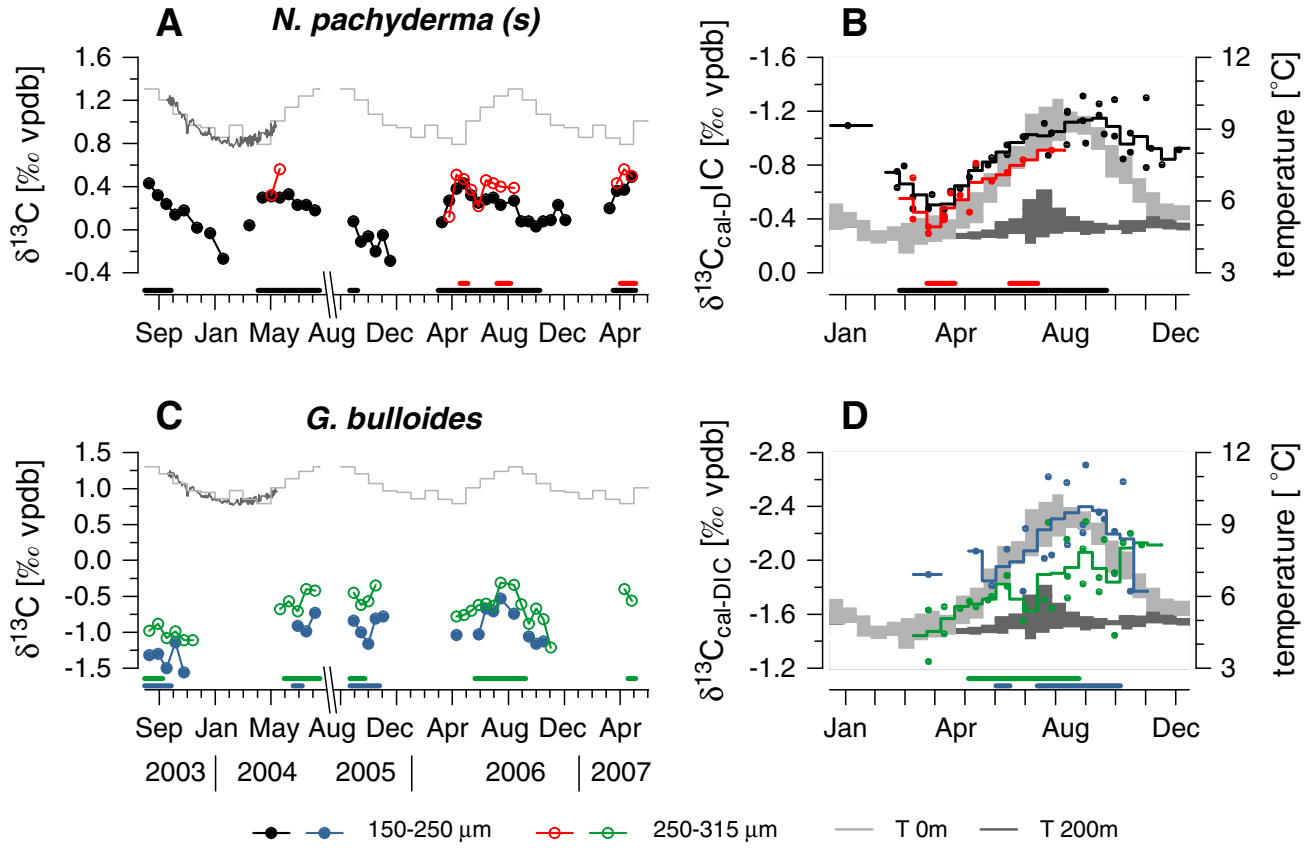

Figure 4. Stable carbon isotopes of *N. pachyderma* (s) and *G. bulloides* compared to $\delta^{13}C_{DIC}$ and temperature. (A and C) Complete foraminiferal $\delta^{13}C$ time-series compared to $\delta^{13}C_{DIC}$; (B and D) annual composites of the offset from $\delta^{13}C_{DIC}$ compared to temperature. In Figures 4A and 4C $\delta^{13}C_{DIC}$ estimates based on WOA09 and CIS data are in light and dark grey respectively. Note different *y*-axis scales for the two species and that the $\delta^{13}C_{cal\text{-}DIC}$ axes are reversed in Figures 4B and 4D to better visualize the coherence between temperature and $\delta^{13}C_{cal\text{-}DIC}$. Thick horizontal lines just above the *x*-axis indicate periods when the shell fluxes were $\geq 10/m^2/d$.

$\delta^{13}C_{DIC}$ increases with calcification temperature and with $[CO_3^{2-}]$ (Figure 5). Ignoring two anomalously low $\delta^{18}O$ values of small *N. pachyderma* (s) from midwinter and a single anomalously high value from large *G. bulloides*, the slopes of the offsets are approximately −0.17‰/°C and −0.016‰/µmol/kg for all species, except for large *G. bulloides* in the case of $[CO_3^{2-}]$ (Figure 5). The relationships are stronger for *N. pachyderma* (s) and also between the $\delta^{13}C_{cal\text{-}DIC}$ and temperature.

4. Discussion

4.1. Flux Timing

[23] Settling fluxes of large and small shells of *N. pachyderma* (s) and *G. bulloides* in the Irminger Sea show clear seasonal patterns. From December to March all fluxes are virtually zero and production occurs during the remaining period of the year (Figure 2). Proxy records will thus be weighted toward the spring to autumn season, barring the reconstruction of wintertime phenomena such as deep-water formation. Little is known about the flux of *N. pachyderma* (s) in the North Atlantic. In the Nordic Seas maximum fluxes are generally equal or larger (>2000 shells/m^2/d) than in the Irminger Sea [*Jensen*, 1998; *Kohfeld et al.*, 1996; *Wolfteich*, 1994]. *N. pachyderma* (s) often dominates assemblages at low temperatures and is probably at the warm end of its temperature habitat in the Irminger Sea [*Tolderlund and Bé*, 1972], which is in agreement with its relatively low fluxes. Importantly, abundances of *N. pachyderma* (s) show a bimodal pattern in the northern North Atlantic, similar to our observations in 2006 [*Tolderlund and Bé*, 1972]. Fluxes of *G. bulloides* in the Eastern North Atlantic north of 50°N are generally comparable to those in the Irminger Sea (<10^2 shells/m^2/d) [*Chapman*, 2010; *Wolfteich*, 1994]. Further south however, the magnitude increases (10^2–10^3 shells/m^2/d) and the season of highest flux shifts toward winter [*Tolderlund and Bé*, 1972; *Wolfteich*, 1994].

[24] The exact timing of the flux pulses of the two species and of the two size fractions depends on the time correction for production and settling. The applied uniform one-month lag for all fluxes might appear to be a crude estimate. However, estimates of the settling speed of foraminiferal shells differ widely and for the size fractions investigated here overlap (40–600 m/d) [*Takahashi and Be*, 1984]. Using sinking speeds of 189–372 m/d for small, and 398–450 m/d

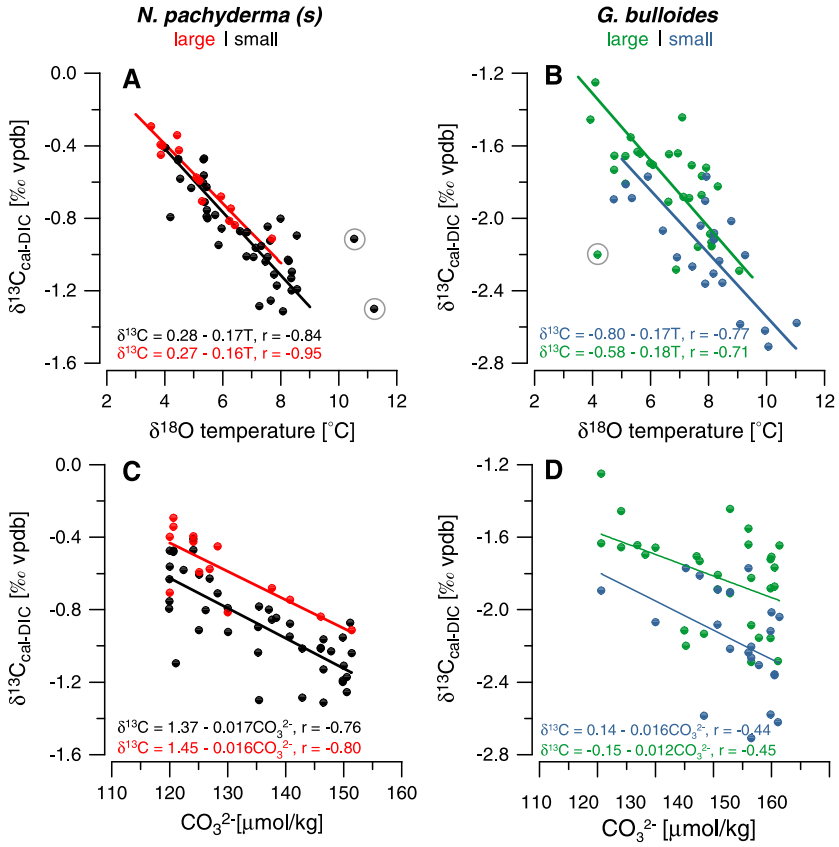

Figure 5. Controls on $\delta^{13}C_{cal\text{-}DIC}$. Scatter plots of $\delta^{13}C_{cal\text{-}DIC}$ vs calcification temperature calculated according to equation (1) for (A) *N. pachyderma* (s) and (B) *G. bulloides* and (C, D) vs. $[CO_3^{2-}]$. Grey circles indicate anomalous temperature estimates during low flux periods that were omitted from regression analysis.

for large shells [*Von Gyldenfeldt et al.*, 2000], the difference in settling time between the size fractions is between 0 and 9 days. Given the uncertainties in the sinking speeds, the 16–19 day resolution of the time series and the variable life span of foraminifera, the uniform lag applied here is therefore reasonable. The duration of the production period is also different for both size fractions with the time of high shell fluxes of large *N. pachyderma* (s) particularly short in comparison to the small shell fluxes (Figure 2). We therefore consider the observed early pulse of large shells to be a real feature of our records (Figure 2). Small *N. pachyderma* (s) fluxes are maintained throughout the production period, but only in spring are conditions favorable enough to allow the production of larger shells of this species (Figure 2). Because the shape of the large shell flux pattern differs from that of the small shells, and the

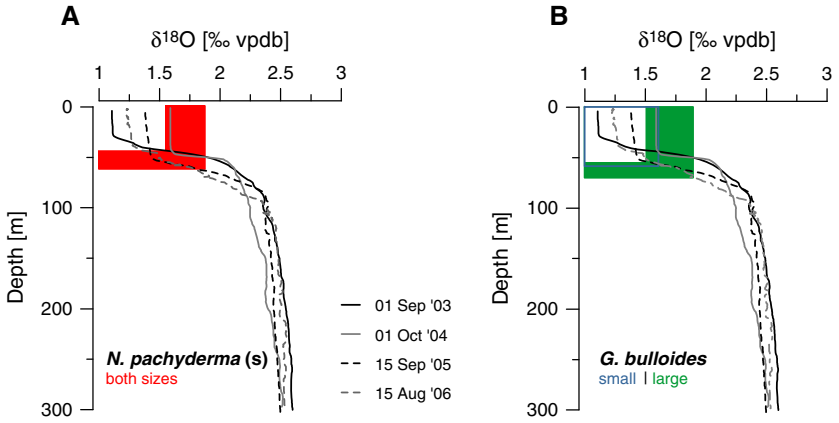

Figure 6. Depth habitat of (A) *N. pachyderma* (s) and (B) *G. bulloides* inferred from $\delta^{18}O$. Profiles of $\delta^{18}O_{eq}$ compared to the observed foraminiferal $\delta^{18}O$ values of at the time of CTD profiling.

magnitude of the flux is approximately an order of magnitude lower, the larger shells probably do not represent further matured specimens, but more likely reflect optimum growth conditions for this species [*Deuser et al*., 1981]. Similarly, the large tests of *G. bulloides* settle earlier in the year, although both size fractions show comparable shapes in the seasonal flux pattern (Figure 2).

[25] The flux of *N. pachyderma* (s) rapidly increases in March, 1 to 2 months prior to the onset of stratification (Figure 2). The flux of small shells of this species remains high and may show a second maximum around the time of the sea surface temperature (stratification) maximum (August; Figure 2). Large shells fluxes generally decrease following the spring bloom in April–May (Figure 2). The flux increase before the onset of stratification as well as the difference in the patterns between large and small shells, suggest that temperature driven stratification changes do not control the seasonal flux of *N. pachyderma* (s). *Jonkers et al*. [2010a] instead highlighted the availability of light and its role in food production as a control on flux timings. However, eddy-driven local stratification may also account for the early start of the springbloom [*Mahadevan et al*., 2012]. Fluxes of *G. bulloides* seem to be more directly controlled by temperature, but with small and large specimens responding slightly differently, leading to large shells settling earlier in the season than small ones (Figure 2). The exact mechanisms causing seasonal differences in different sized shells and those responsible for the bimodal flux pattern of small *N. pachyderma* (s) remain as yet poorly understood. Ecological models do not currently resolve these (size-related) patterns [*Fraile et al*., 2008; *Lombard et al*., 2011], limiting our ability to assess the effects of transient seasonality changes on planktonic foraminiferal proxy records.

4.2. δ^{18}O-Depth

[26] Both species calcify without an offset from $\delta^{18}O_{eq}$, thus the shell $\delta^{18}O$ can be used to directly estimate calcification depth using the water column profiles of $\delta^{18}O_{eq}$. Such profiles from late summer and autumn indicate that the $\delta^{18}O$ of large and small *N. pachyderma* (s) from the same period reflects seawater $\delta^{18}O$ over the same narrow zone just below the surface mixed layer, around 50 m depth (Figure 6A). For *G. bulloides* the size-related $\Delta\delta^{18}O_{s-l}$ is close its maximum during this same period, resulting in an upper estimate of the depth habitat differences (Figure 4B). Small *G. bulloides* reflect temperatures in the upper 50 m, including the mixed layer, whereas large shells reflect thermocline temperatures only (Figure 6B). The divergence from surface $\delta^{18}O_{eq}$ seen in all shells except small *G. bulloides* (Figure 3), is in agreement with a depth habitat below the surface where the amplitude of $\delta^{18}O_{eq}$ is slightly muted compared to at 0 m depth (Figure 1).

[27] The estimated calcification depth of ~50 m in the thermocline for *N. pachyderma* (s) is shallower than often reported [*Bauch et al*., 1997; *Simstich et al*., 2003], but the amplitude of the $\delta^{18}O$ signal as well as the absolute values recorded here are in good agreement with this inferred depth (Figure 3). This species is known to adjust its depth habitat in response to local hydrography, which is probably the main reason why the estimates of its depth habitat differ regionally [*Jonkers et al*., 2010a; *Kohfeld et al*., 1996; *Simstich et al*., 2003]. Different ecological preferences as a result of genotypic variability within *N. pachyderma* (s) [*Bauch et al*., 2003] may also contribute to the different depth habitats observed in different regions, but this cannot be verified here. This depth habitat variability complicates reconstructions based on this species, particularly across intervals accompanied by changes in the density structure of the upper water column.

[28] The $\delta^{18}O$ of small *N. pachyderma* (s) is below surface $\delta^{18}O_{eq}$ when fluxes are near zero between November and January (Figures 2 and 3). *Jonkers et al*. [2010a] suggested that these low values were due to remnants of the summer population that survived in the upper water column without actively calcifying. These shells have therefore retained a $\delta^{18}O$ signal associated with the preceding summer.

[29] In *G. bulloides* the differences between the $\delta^{18}O$ of large and small shells (Figure 3) could be due to vital/ontogenetic effects [*Bemis et al*., 1998; *Peeters et al*., 2002],

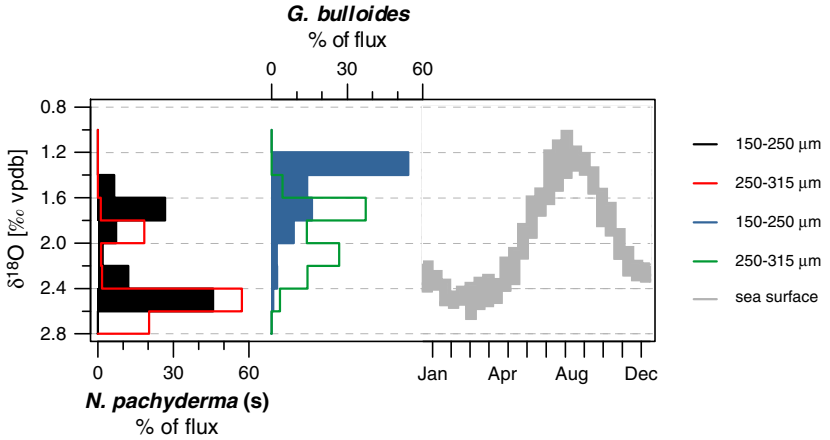

Figure 7. Seasonality effect on flux-weighted $\delta^{18}O$. The colored bars show flux-weighted $\delta^{18}O$ histograms and the grey curve is the sea surface $\delta^{18}O_{eq}$ as shown in Figure 3. Largest $\Delta\delta^{18}O$, and thus an improved estimate of seasonal stratification, can be obtained when large *N. pachyderma* (s) and small *G. bulloides* are analyzed in parallel.

but in the Irminger Sea more likely reflect a combination of these effects as well as differentiation in the depth habitat of larger and smaller shells. Two lines of reasoning support this; (I) the higher amplitude of the $\delta^{18}O$ of small shells is consistent with a shallower habitat where temperature changes are larger than at depth, and (II) a different depth habitat for the two size classes can explain the progressive increase in the $\Delta\delta^{18}O_{s\text{-}l}$ during the season because the temperature difference between the two depth zones increases with increasing stratification.

4.3. Size Effects on $\delta^{18}O$

[30] The data do not show a consistent size effect on the $\delta^{18}O$ of *N. pachyderma* (s) in the Irminger Sea (Figure 3). However, in other areas, larger shells collected by plankton tows or from sediment traps generally show more positive values than smaller foraminifera (up to 0.79‰ difference between 125–180 and 180–250 μm in the North Pacific [*Kuroyanagi et al*., 2011]), suggesting that larger *N. pachyderma* (s) either calcify deeper in the water column, or with a different offset from equilibrium than smaller ones [*Bauch et al*., 1997; *Donner and Wefer*, 1994; *Kuroyanagi et al*., 2011]. The hydrographic and/or nutrient/food conditions in the Irminger Sea probably prevent depth habitat differentiation of this species, resulting in similar $\delta^{18}O$ in small and large shells. Thus, any differences between the two size classes in fossil specimens from this area, most likely reflect growth at different times of the year.

[31] The size effect on $\delta^{18}O$ in *G. bulloides* is larger and intra-annually and interannually more variable than in *N. pachyderma* (s) (Figure 3). The more positive $\delta^{18}O$ of larger shells agrees well with studies from laboratory cultures and plankton tows [*Bemis et al*., 1998; *Peeters et al*., 2002]. The 0.20‰ difference between shell sizes is also within the reported range, but because the size classes differ amongst studies an absolute comparison cannot be made.

4.4. Seasonality Effects on $\delta^{18}O$

[32] For accurate interpretation of fossil foraminiferal $\delta^{18}O$, the flux-weighted mean $\delta^{18}O$ of the sediment trap data is important, because this determines the signal that is preserved in the sediment. Note that the flux-weighted values are independent of any assumptions on the time lag for settling and production. In both species large shells settle earlier in the season, thereby recording lower temperatures than the small shells (Figure 7). The sediment trap data do not show a systematic size-related difference in the $\delta^{18}O$ of *N. pachyderma* (s). Therefore, the flux-weighted average of large minus that of the small shells ($\Delta\delta^{18}O_{s\text{–}l}$) solely reflects the difference in seasonality between the size classes. The flux-weighted $\Delta\delta^{18}O_{s\text{–}l}$ in *N. pachyderma* (s) amounts to 0.29 ‰, equivalent to approximately a 1.2°C lower estimated temperature for the large shells. In *G. bulloides*, where there is a difference between small and large shells, the flux-weighted $\Delta\delta^{18}O_{s\text{–}l}$ is 0.48 ‰, more than double the average size-related $\Delta\delta^{18}O_{s\text{–}l}$ of 0.20‰ and roughly equivalent to a 1.9°C difference in estimated temperature. In this species, the total flux-weighted $\Delta\delta^{18}O_{s\text{-}l}$ thus reflects a combination of size and seasonality effects, of approximately 0.20 ‰ and 0.28 (0.48–0.20) ‰, respectively.

[33] The fossil $\Delta\delta^{18}O$ between *N. pachyderma* (s) and *G. bulloides* has been used to estimate changes in the stratification of the upper water column in the past [*Hillaire-Marcel et al*., 2001]. Such estimates can potentially be improved by taking into account the differences in seasonality between large and small shells (Figure 7). The flux-weighted interspecies $\Delta\delta^{18}O_{pac\text{-}bul}$ for small and large shells is 0.66 and 0.48‰, respectively, whereas the seasonal surface $\delta^{18}O_{eq}$ amplitude is 1.29‰. Taking advantage of the early production of large *N. pachyderma* (s) shells and the late timing of small *G. bulloides* the $\Delta\delta^{18}O_{pac\ l\text{-}bul\ s}$ increases to 0.95‰, providing a seasonality estimate that is considerably closer to the annual $\delta^{18}O_{eq}$ amplitude (Figure 7). Note also that due to the single high flux event in large *N. pachyderma* (s) in July 2006 the flux-weighted mean is skewed toward the summer, the sedimentary $\delta^{18}O$ may therefore more closely reflect winter and early spring conditions, providing an even larger $\Delta\delta^{18}O_{pac\ l\text{-}bul\ s}$ (Figures 2 and 7). While the difference in flux timing between size fractions varies regionally [*Kuroyanagi et al*., 2011; *Reynolds and Thunell*, 1985; *Thunell and Reynolds*, 1984] these are the first data from the northern North Atlantic that suggest that the flux- and size-weighted $\Delta\delta^{18}O$ could be used as an indicator of past seasonal changes in the stratification of the upper water column.

4.5. Interspecies and Intraspecies $\Delta\delta^{13}C$

[34] The $\delta^{13}C$ of *G. bulloides* is on average >1‰ lower than that of *N. pachyderma* (s), whereas the difference between the size fractions is much smaller (0.28‰ *G. bulloides*; 0.12‰ *N. pachyderma* (s)). Of the four main factors that can cause differences in $\delta^{13}C$, symbiotic activity can be excluded as neither species bears symbionts [*Hemleben et al*., 1989]. The $\delta^{18}O$ values indicate that large *G. bulloides* and *N. pachyderma* (s) form simultaneously within the same depth zone (Figure 3). Consequently, neither temperature or carbonate system parameters can be responsible for the interspecies $\Delta\delta^{13}C$. Species-specific ontogenetic/metabolic effects must therefore be the most important cause of the observed difference in $\delta^{13}C$ between *N. pachyderma* (s) and *G. bulloides*.

[35] The same reasoning leads to the conclusion that the difference between large and small *N. pachyderma* (s) must also be predominantly due to ontogenetic/metabolic effects [*Kohfeld et al*., 1996]. *G. bulloides*, however, shows a clearer separation of depth habitats between size fractions and a larger and more variable size-related $\Delta\delta^{13}C$ (Figure 4). Size-related differences, due to metabolism/ontogeny are known to affect the carbon isotopic composition, causing larger tests to have higher $\delta^{13}C$ values [*Bemis et al*., 2000; *Spero and Lea*, 1996]. However, the influence of temperature and carbon system parameters at the different depth zones cannot be readily evaluated with the present data set, but may also play a role in explaining the variable differences between the size fractions in *G. bulloides*.

4.6. Seasonal $\delta^{13}C$ Change

[36] The seasonally variable offset from $\delta^{13}C_{DIC}$ for both species indicates that so-called vital effects cause the foraminiferal $\delta^{13}C$ to deviate from $\delta^{13}C_{DIC}$ (Figures 4B and 4D). Temperature and $[CO_3^{2-}]$ have both been shown to have an influence on this offset from $\delta^{13}C_{DIC}$ [*Bauch et al*., 2002; *Bemis et al*., 2000; *Spero et al*., 1997]. In the training area for our MLR and in the wider North Atlantic region

temperature and $[CO_3^{2-}]$ are however strongly positively correlated ($r = 0.94$, not shown), yielding it difficult to distinguish their respective influences on foraminiferal $\delta^{13}C$. Nevertheless, the slopes of the temperature dependence of $\delta^{13}C_{cal\text{-}DIC}$ (Figure 5A, B) are virtually identical to that observed for *G. bulloides* collected in the northwestern Pacific [*Bemis et al*., 2000]. Moreover, using a very different approach *Kohfeld et al.* [2000] calculate offsets from $\delta^{13}C_{DIC}$ of *N. pachyderma* (s) in sediments in the South Atlantic and derive a temperature dependence of $\delta^{13}C_{cal\text{-}DIC}$ (−0.16‰/°C) strikingly similar to that in the Irminger Sea (Figure 5). Culturing of *G. bulloides* under controlled laboratory conditions yielded gentler slopes (−0.11 vs. –0.18‰/°C) [*Bemis et al*., 2000], suggesting that there is some variability in the sensitivity of $\delta^{13}C_{cal\text{-}DIC}$ to temperature between regions and/or between (genetically) different populations. Nevertheless, the similarity of the slope to other studies, in conjunction with the higher correlation coefficient (Figure 5), suggests that temperature has a stronger control on the $\delta^{13}C_{cal\text{-}DIC}$ than $[CO_3^{2-}]$ in the Irminger Sea. This temperature sensitivity of ~0.17‰/°C of foraminiferal $\delta^{13}C$ is close to that of $\delta^{18}O$ (~0.25‰/°C) and warrants reinterpretation of foraminiferal $\delta^{13}C$ records previously interpreted as nutrient or ventilation changes [e.g., *Jonkers et al*., 2010b; *Van Kreveld et al*., 2000]. The scatter in the temperature- $\delta^{13}C_{cal\text{-}DIC}$ relationship as well as the different $\delta^{13}C_{cal\text{-}DIC}$ patterns for shells grown at the same depth indicate that ontogenetic/metabolic effects also have an impact on the seasonal $\delta^{13}C$ patterns of both species and controlled experiments are needed to firmly disentangle the respective influences of temperature and $[CO_3^{2-}]$ on the foraminiferal offset from seawater $\delta^{13}C_{DIC}$. Irrespective of the exact control on the $\delta^{13}C_{cal\text{-}DIC}$, its seasonal variability means that fossil foraminiferal $\delta^{13}C$ reflects $\delta^{13}C_{DIC}$ with an offset that is not only determined by temperature or $[CO_3^{2-}]$, but also by timing of the flux during the year.

5. Conclusions

[37] The data from the 2.5 year time series from the Irminger Sea indicate:

[38] 1. That the seasonal flux patterns of *N. pachyderma* (s) and *G. bulloides* are not primarily controlled by temperature (and hence stratification) because flux patterns differ for different size fractions, and in the case of *N. pachyderma* (s), appear bimodal and start before the onset of stratification. The two species show a difference in their seasonality: shells of *N. pachyderma* (s) settle earlier in the season than those of *G. bulloides*. In both species large shells (250–315 μm) are formed earlier in the season than small shells (150–250 μm).

[39] 2. Both species' $\delta^{18}O$ are indistinguishable from inorganically precipitated calcite, i.e., they do not show an offset from $\delta^{18}O$ predicted according to *Kim and O'Neil* [1997]. Using this information we estimate a shallow (<~50 m) habitat for both species and no depth habitat differentiation between small and large *N. pachyderma* (s). The $\delta^{18}O$ of large *G. bulloides* shells however, reflects $\delta^{18}O$ slightly deeper in the water column than small shells.

[40] 3. Differences in seasonality between the species and size classes cause the flux-weighted $\delta^{18}O$ to reflect different periods in the year, with large *N. pachyderma* (s) reflecting the coldest, early spring conditions and small *G. bulloides* biased toward warm summer conditions. In the region the difference in seasonality between size classes could potentially be used to obtain a more robust estimate of seasonal stratification from fossil interspecies $\Delta\delta^{18}O$ than when comparing $\delta^{18}O$ values in the same size range.

[41] 4. *N. pachyderma* (s) $\delta^{13}C$ are, throughout the season, approximately ~1 ‰ higher than *G. bulloides*. This difference is attributed to species-specific ontogenetic/metabolic effects. Similar effects are probably responsible for the observed differences between small and large shells of both species (large 0.12-0.28 ‰ > small). In both species the seasonally variable offset from seawater $\delta^{13}C_{DIC}$ appears to be to a large degree controlled by temperature, but since sea water temperature and $[CO_3^{2-}]$ strongly correlate, this conclusion requires further research. The seasonal variation in the offset from $\delta^{13}C_{DIC}$, however, implies that fossil $\delta^{13}C$ also depends on the seasonality of the foraminifera, further implicating the use of planktonic foraminiferal $\delta^{13}C$ in paleoceanography.

[42] **Acknowledgments**. L.J. received funding from the European Community's Seventh Framework Programme FP7/2007-2013 – Marie-Curie ITN, under grant agreement n° 238512, GATEWAYS project. The mooring deployment was supported financially through VAMOC RAPiD NWO-ALW 854 00 020. We thank Geert-Jan Brummer for making the sediment trap samples available, Pati Jiménez-Amat for help with laboratory work and Kirsty Edgar for correcting the English. Helpful comments by two anonymous reviewers and the associate editor D. Schmidt are thankfully acknowledged.

References

Antonov, J. I., D. Seidov, T. P. Boyer, R. A. Locarnini, A. V. Mishonov, H. E. Garcia, O. K. Baranova, M. M. Zweng, and D. R. Johnson (2010), World Ocean Atlas 2009, Volume 2: Salinity, in NOAA Atlas NESDIS 69, edited by S. Levitus, p. 184, U.S. Government Printing Office, Washington D.C.

Bacon, S., W. J. Gould, and Y. Jia (2003), Open-ocean convection in the Irminger Sea, *Geophys. Res. Lett.*, *30*(5), 1246, doi:1210.1029/2002GL016271.

Bauch, D., J. Carstens, and G. Wefer (1997), Oxygen isotope composition of living *Neogloboquadrina pachyderma* (sin.) in the Arctic Ocean, *Earth Planet. Sci. Lett.*, *146*(1–2), 47–58.

Bauch, D., K. Darling, J. Simstich, H. A. Bauch, H. Erlenkeuser, and D. Kroon (2003), Palaeoceanographic implications of genetic variation in living North Atlantic Neogloboquadrina pachyderma, *Nature*, *424* (6946), 299–302.

Bauch, D., H. Erlenkeuser, G. Winckler, G. Pavlova, and J. Thiede (2002), Carbon isotopes and habitat of polar planktic foraminifera in the Okhotsk Sea: the 'carbonate ion effect' under natural conditions, *Mar. Micropaleontol.*, *45*(2), 83–99.

Bemis, B. E., H. J. Spero, J. Bijma, and D. W. Lea (1998), Reevaluation of the Oxygen Isotopic Composition of Planktonic Foraminifera: Experimental Results and Revised Paleotemperature Equations, *Paleoceanography*, *13* (2), 150–160.

Bemis, B. E., H. J. Spero, D. W. Lea, and J. Bijma (2000), Temperature influence on the carbon isotopic composition of *Globigerina bulloides* and *Orbulina universa* (planktonic foraminifera), *Mar. Micropaleontol.*, *38*(3–4), 213–228.

Berger, W. H., J. S. Killingley, and E. Vincent (1978), Stable isotopes in deep-sea carbonates: Box core ERDC-92, west equatorial Pacific, *Oceanol. Acta*, *1*(2), 203–216.

Billups, K., and H. J. Spero (1995), Relationship between shell size, thickness and stable isotopes in individual planktonic foraminifera from two Equatorial Atlantic cores, *J. Foraminifer. Res.*, *25*(1), 24–37.

Bouvier-Soumagnac, Y., and J.-C. Duplessy (1985), Carbon and oxygen isotopic composition of planktonic foraminifera from laboratory culture, plankton tows and Recent sediment; implications for the reconstruction of paleoclimatic conditions and of the global carbon cycle, *J. Foraminifer. Res.*, *15*(4), 302–320.

Broecker, W. S., and E. Maier-Reimer (1992), The influence of air and sea exchange on the carbon isotope distribution in the sea, *Global Biogeochem. Cycles*, *6*(3), 315–320.

Broecker, W. S., and T. H. Peng (1982), Tracers in the Sea, 689 pp., Eldigio Press, Lamont-Doherty Geological Observatory of Columbia University, Palisades, NY.

Chapman, M. R. (2010), Seasonal production patterns of planktonic foraminifera in the NE Atlantic Ocean: Implications for paleotemperature and hydrographic reconstructions, *Paleoceanography*, *25*(PA1101), doi:10.1029/2008PA001708.

Deuser, W. G., E. H. Ross, C. Hemleben, and M. Spindler (1981), Seasonal changes in species composition, numbers, mass, size, and isotopic composition of planktonic foraminifera settling into the deep sargasso sea, *Palaeogeogr. Palaeoclimatol. Palaeoecol.*, *33*(1–3), 103–127.

Donner, B., and G. Wefer (1994), Flux and stable isotope composition of *Neogloboquadrina pachyderma* and other planktonic foraminifers in the Southern Ocean (Atlantic sector), *Deep-Sea Res. I Oceanogr. Res. Pap.*, *41*(11–12), 1733–1743.

Field, D. B. (2004), Variability in vertical distributions of planktonic foraminifera in the California Current: Relationships to vertical ocean structure, *Paleoceanography*, *19*(2), PA2014.

Fraile, I., M. Schulz, S. Mulitza, and M. Kucera (2008), Predicting the global distribution of planktonic foraminifera using a dynamic ecosystem model, *Biogeosciences*, *5*(3), 891–911.

Garcia, H. E., R. A. Locarnini, T. P. Boyer, J. I. Antonov, M. M. Zweng, O. K. Baranova, and D. R. Johnson (2010), World Ocean Atlas 2009, Volume 4: Nutrients (phosphate, nitrate, silicate), in NOAA Atlas NESDIS 71, edited by S. Levitus, p. 398, U.S. Government Printing Office, Washington D.C.

Gruber, N., C. D. Keeling, R. B. Bacastow, P. R. Guenther, T. J. Lueker, M. Wahlen, H. A. J. Meijer, W. G. Mook, and T. F. Stocker (1999), Spatiotemporal patterns of carbon-13 in the global surface oceans and the oceanic suess effect, *Global Biogeochem. Cycles*, *13*(2), 307–335.

Hemleben, C., M. Spindler, and O. R. Anderson (1989), Modern Planktonic Foraminifera, Springer, Verlag.

Hillaire-Marcel, C., A. de Vernal, G. Bilodeau, and A. J. Weaver (2001), Absence of deep-water formation in the Labrador Sea during the last interglacial period, *Nature*, *410*(6832), 1073–1077.

Hut, G. (1987), Consultants'Group Meeting on Stable Isotope Reference Samples for Geochemical and Hydrological Investigations, *International Atomic Energy Agency*, *42* pp.

Jensen, S. (1998), Planktische Foraminiferen im Europäischen Nordmeer: Verbreitung und Vertikalfluss sowie ihre Verbreitung während der letzten 15,000 Jahre, *Berichte Sonderforschungsbereich 313*(75), 1–105.

Jonkers, L., G.-J. A. Brummer, F. J. C. Peeters, H. M. van Aken, and M. F. De Jong (2010a), Seasonal stratification, shell flux, and oxygen isotope dynamics of left-coiling *N. pachyderma* and *T. quinqueloba* in the western subpolar North Atlantic, *Paleoceanography*, *25*(2), PA2204; doi:2210.1029/2009PA001849.

Jonkers, L., M. Moros, M. A. Prins, T. M. Dokken, N. Dijkstra, K. Perner, and G. J. A. Brummer (2010b), A reconstruction of sea surface warming in the northern North Atlantic during MIS 3 ice-rafting events, *Quat. Sci. Rev.*, doi:10.1016/j.quascirev.2010.1003.1014.

Key, R. M., A. Kozyr, C. L. Sabine, K. Lee, R. Wanninkhof, J. L. Bullister, R. A. Feely, F. J. Millero, C. Mordy, and T. H. Peng (2004), A global ocean carbon climatology: Results from Global Data Analysis Project (GLODAP), *Global Biogeochem. Cycles*, *18*(4), GB4031.

Key, R. M., et al. (2010), The CARINA data synthesis project: introduction and overview, *Earth Syst. Sci. Data*, *2*(1), 105–121.

Kim, S.-T., and J. R. O'Neil (1997), Equilibrium and nonequilibrium oxygen isotope effects in synthetic carbonates, *Geochim. Cosmochim. Acta*, *61*(16), 3461–3475.

Kohfeld, K. E., R. F. Anderson, and J. Lynch-Stieglitz (2000), Carbon Isotopic Disequilibrium in Polar Planktonic Foraminifera and Its Impact on Modern and Last Glacial Maximum Reconstructions, *Paleoceanography*, *15*(1), 53–64.

Kohfeld, K. E., R. G. Fairbanks, S. L. Smith, and I. D. Walsh (1996), *Neogloboquadrina pachyderma* (sinistral coiling) as Paleoceanographic Tracers in Polar Oceans: Evidence from Northeast Water Polynya Plankton Tows, Sediment Traps, and Surface Sediments, *Paleoceanography*, *11*(6), 679–699.

Kuroyanagi, A., H. Kawahata, and H. Nishi (2011), Seasonal variation in the oxygen isotopic composition of different-sized planktonic foraminifer *Neogloboquadrina pachyderma* (sinistral) in the northwestern North Pacific and implications for reconstruction of the paleoenvironment, *Paleoceanography*, *26*(4), PA4215.

Locarnini, R. A., A. V. Mishonov, J. I. Antonov, T. P. Boyer, H. E. Garcia, O. K. Baranova, M. M. Zweng, and D. R. Johnson (2010), World Ocean Atlas 2009, Volume 1: Temperature, in NOAA Atlas NESDIS 68, edited by S. Levitus, p. 184, U.S. Government Printing Office, Washington, D.C.

Lombard, F., L. Labeyrie, E. Michel, L. Bopp, E. Cortijo, S. Retailleau, H. Howa, and F. Jorissen (2011), Modelling planktic foraminifer growth and distribution using an ecophysiological multi-species approach, *Biogeosciences*, *8*(4), 853–873.

Mahadevan, A., E. D'Asaro, C. Lee, and M. J. Perry (2012), Eddy-Driven Stratification Initiates North Atlantic Spring Phytoplankton Blooms, *Science*, *337*(6090), 54–58.

Mulitza, S., A. Duerkoop, W. Hale, G. Wefer, and H. S. Niebler (1997), Planktonic foraminifera as recorders of past surface-water stratification, *Geology*, *25*(4), 335–338.

Peeters, F. J. C., G.-J. A. Brummer, and G. Ganssen (2002), The effect of upwelling on the distribution and stable isotope composition of *Globigerina bulloides* and *Globigerinoides ruber* (planktic foraminifera) in modern surface waters of the NW Arabian Sea, *Glob. Planet. Chang.*, *34*(3–4), 269–291.

Quay, P., R. Sonnerup, J. Stutsman, J. Maurer, A. Körtzinger, X. A. Padin, and C. Robinson (2007), Anthropogenic CO2 accumulation rates in the North Atlantic Ocean from changes in the 13C/12C of dissolved inorganic carbon, *Global Biogeochem. Cycles*, *21*(1), GB1009.

Ravelo, A. C., and R. G. Fairbanks (1995), Carbon isotopic fractionation in multiple species of planktonic foraminifera from core-tops in the tropical Atlantic, *J. Foraminifer. Res.*, *25*(1), 53–74.

Reynolds, L., and R. Thunell (1985), Seasonal succession of planktonic foraminifera in the subpolar North Pacific, *J. Foraminifer. Res.*, *15*(4), 282–301.

Simstich, J., M. Sarnthein, and H. Erlenkeuser (2003), Paired $\delta^{18}O$ signals of *Neogloboquadrina pachyderma* (s) and *Turborotalita quinqueloba* show thermal stratification structure in Nordic Seas, *Mar. Micropaleontol.*, *48*(1–2), 107–125.

Spero, H. J., and D. W. Lea (1996), Experimental determination of stable isotope variability in Globigerina bulloides: implications for paleoceanographic reconstructions, *Mar. Micropaleontol.*, *28*(3–4), 231–246.

Spero, H. J., J. Bijma, D. W. Lea, and B. E. Bemis (1997), Effect of seawater carbonate concentration on foraminiferal carbon and oxygen isotopes, *Nature*, *390*(6659), 497–500.

Takahashi, K., and A. W. H. Be (1984), Planktonic foraminifera: factors controlling sinking speeds, *Deep Sea Research Part A. Oceanographic Research Papers*, *31*(12), 1477–1500.

Thunell, R. C., and L. A. Reynolds (1984), Sedimentation of planktonic foraminifera; seasonal changes in species flux in the Panama Basin, *Micropaleontology*, *30*(3), 243–262.

Tolderlund, D. S., and A. W. H. Bé (1972), Seasonal distribution of planktonic foraminifera in the western North Atlantic, *Micropaleontology*, *17*(3), 297–329.

van Heuven, S., D. Pierrot, J. W. B. Rae, E. Lewis, and D. W. R. Wallace (2009), MATLAB Program Developed for CO_2 System Calculations, *ORNL/CDIAC-105b. Carbon Dioxide Information Analysis Center*, *Oak Ridge National Laboratory*, *U.S. Department of Energy*, *Oak Ridge*, *Tennessee*. (*updated in 2011*).

Van Kreveld, S., M. Sarnthein, H. Erlenkeuser, P. Grootes, S. Jung, M. J. Nadeau, U. Pflaumann, and A. Voelker (2000), Potential links between surging ice sheets, circulation changes, and the Dansgaard-Oeschger cycles in the Irminger Sea, 60–18 kyr, *Paleoceanography*, *15*(4), 425–442.

Von Gyldenfeldt, A.-B., J. Carstens, and J. Meincke (2000), Estimation of the catchment area of a sediment trap by means of current meters and foraminiferal tests, *Deep-Sea Res. II Top. Stud. Oceanogr.*, *47*(9–11), 1701–1717.

Wolfteich, C. M. (1994), Sattelite-derived sea surface temperature, mesoscale variability, and foraminiferal production in the North Atlantic, 91 pp, MSc thesis MIT and WHOI joint program, Cambridge, MA.